Hydrophobic Properties of Polymer Films on Cast Iron Substrates

Materials Characterization

Dewayne Broome and Syndee Villa

May 6, 2020

Abstract:

The properties of hydrophobic surfaces have been of recent interest due to their applications in cookware and automotive components. The wetting properties of surfaces usually have an effect on the frictional forces due to the surface roughness of a material and the degree of wetting it creates. Non-stick in cookware has been used because it is easier to clean, cook, heats the food evenly, and requires less oil each time it is used, which makes it a healthy alternative. For the cookware, the necessity arises from users not wanting food or debris to stick to their surfaces and the automotive necessity arises from car parts needing to maintain their tolerances in order for them to function properly. This study aims to explore the surface chemistry properties of cast iron in these applications where we measure contact angles between water molecules, observe the microstructure, and measure frictional and adhesion forces to a grey cast iron sample with deposited oil layer. Our main goal is to design and quantify the hydrophobic properties of a cast iron surface.

Introduction:

Grey cast iron is considered the cheapest engineering metal. Casting cast iron is very easy since it is more fluid and has a narrower solidification range than steel. Grey cast iron is named after its grey fractured surface that occurs because the graphitic flakes deflect a passing crack and initiate countless new cracks as the material breaks. Therefore, its strength and ductility characteristics move engineers to develop more applications for grey cast iron. Grey cast iron is very essential in the engineering world and especially in cookware. Nonstick pans and pots are constantly needed and the nonstick provided by grey cast iron and other characteristics makes it a perfect fit for the application. A non-stick surface reduces the ability of other materials to stick

to it. Non-stick cookware allows food to brown without sticking it to the pan (Cabello, 2017). Non-stick pans are often coated with polytetrafluoroethylene. Other coatings have been used for nonstick such as anodized aluminum, ceramics, silicone, and seasoned cookware. Grey cast iron is by far the oldest and most common form of cast iron. The flakes of graphite have good damping characteristics and good machinability because the graphite acts as a chip breaker and lubricates the cutting tools. In applications involving wear, the graphite is beneficial because it helps retain lubricants. A final benefit of grey cast iron is its ability to withstand thermal cycling well. Thermal cycling is where the component changes from warmer and colder temperatures. While grey cast iron has less strength and shock resistance than steel, it also has compressive strength that is compared to low and medium carbon steel. The purpose of investigating carbon for automotive parts was to analyze the correlation between corrosion and hydrophobicity. Corrosion of metals is a destructive reaction towards the material and can cause the product to not function properly and fail much sooner than intended (Ramachadran).

Scanning electron microscopes are capable of imaging at high resolution and a large depth of field. A benefit of a large depth of field is a total surface profile of the sample that is being imaged. This instrument is mostly used to obtain topographic data. Using a Through- the-lens and Everhart-Thornley detector for secondary electrons creates a surface image. The different samples we will be observing is a vegetable cast iron, olive oil seasoned cast iron, bare cast iron, and cast iron. With the SEM we will use a certain type of scan called an area scan. With an area scan the SEM will be observing the sample within a set of corresponding locations. Observing an area instead the entire sample allows precise and specific viewing of areas on the sample which generates topographical images. Using a TTL detector creates a projection of the lens magnetic field onto the sample that attracts secondary electrons that are detected and

improves the resolution. The other intended instruments we plan on using are an optical contact angle goniometer and Atomic Force Microscopy (AFM). With AFM, we will be able to perform force microscopy and be able to manipulate the forces between the tip and the individual samples to change the properties of the sample. For imaging, AFM allows us to form a three-dimensional shape of the samples' surfaces at a high resolution. Also, the AFM measures adhesive and cohesive forces. Since we are also taking into account that we are not working with an ideal smooth surface but one with some surface roughness in order to obtain the calculation for the root mean square value with the AFM. The goniometer tool will allow us to measure the contact angle between the surface and the liquid. Each sample will generate a different contact angle which we will then compare. Also, with the goniometer, we can determine surface tension. A Venn diagram comparison of each technique can be seen in Figure 1.

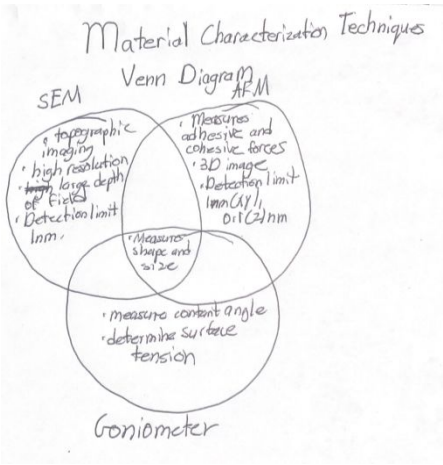

Figure 1. Venn diagram comparing the different techniques that produce different data.

Cast iron has been studied with lubricant addition for its frictional wear characteristics and some non-academic research has been done by cookware enthusiasts. Different treatments have been studied for cast iron cookware where they attempt to investigate which oil or temperature produces the best hydrophobic properties and results. The Lodge Company recommended using a vegetable or canola oil versus animal fat as it may go rancid. Sheryl Canter recommended differently after having conducted her cast iron seasoning experiment where she deduced flaxseed oil as being the best oil to use. It has been presumed by cooking experts that seasoning cast iron skillets will prolong the life of the skillet and also ensure a hydrophobic surface without the need of much oil when cooking. We aim to study the surface properties of cast iron when seasoned with conventional cooking oils such as vegetable oil and olive oil. With the preliminary data we were able to investigate the contact angles of each surface with the different deposited layers. Contact angle measurements through a goniometer via a sessile droplet allows us to gain knowledge about what wetting model is exhibited at the surface. The Wenzel wetting model would indicate a higher surface roughness, higher surface energy, and higher contact angle as this model would indicate complete wetting making this a hydrophilic surface. The Cassie Baxter model would indicate a lower surface roughness, and a lower contact angle as this model would be less hydrophilic and more hydrophobic, as it would describe partial wetting as we would expect for this cast iron skillet once it is treated. The interactions in our material that are expected to contribute to the surface tension are dipole bonds, unlike its London dispersion forces which are much weaker than its dipole-dipole bonding. We would also expect in our contact angle measurements that air exposure to our surfaces could affect the results as seen in a previous study (Riahi, 2017).

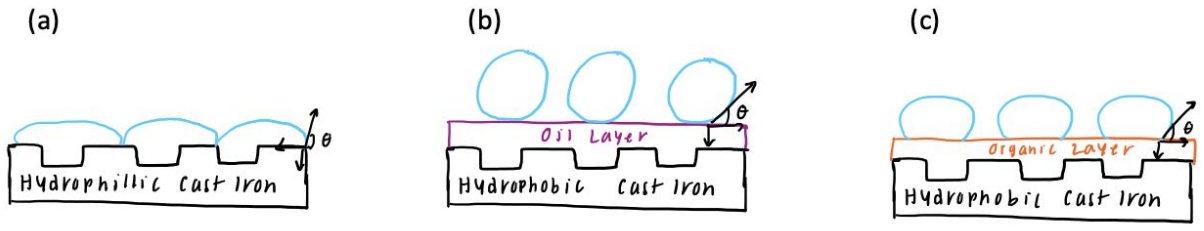

Figure 2. (a) Bare Grey Cast Iron microstructure schematic. (b) Bare Grey Cast Iron after Oil Layer deposition microstructure schematic. (c) Uncleaned Grey Cast Iron with organic layer intact microstructure schematic.

We can see from Figure 2(a) showing our experimental hypothesis for a cleaned grey cast iron surface with isopropyl alcohol, which suggests the rough surface would present as a Wenzel model due to its wettability for water molecules on the surface. Figure 2(b) shows the grey cast iron cleaned with isopropyl alcohol and then forming a polymerized layer through oil polymerization. We can see that Figure 2(b) shows a hydrophobic surface after the oil layer was deposited and polymerized with a high contact angle. Figure 2(c) shows a grey cast iron sample that was not cleaned and allowed for the organic layer to maintain intact; this would also show some hydrophobicity as the organic layer itself could have had a fat polymerization on the substrate, which gave it the hydrophobicity. We can assume that the oil layer gives us a higher contact angle than the organic fat layer. Our hydrophobic surfaces would predict that we would have higher cohesive forces, which would have a higher work of cohesion because the molecules want to stick to themselves instead of the surface. The hydrophilic surfaces predict higher adhesive forces, which then lead us to believe the water molecules want to adhere more to the substrate, making it harder to separate these two different mediums. The Wenzel and Cassie

Baxter models were implemented due to the assumption that multiple layers of the polymer lays could contribute to an uneven surface with some surface roughness.

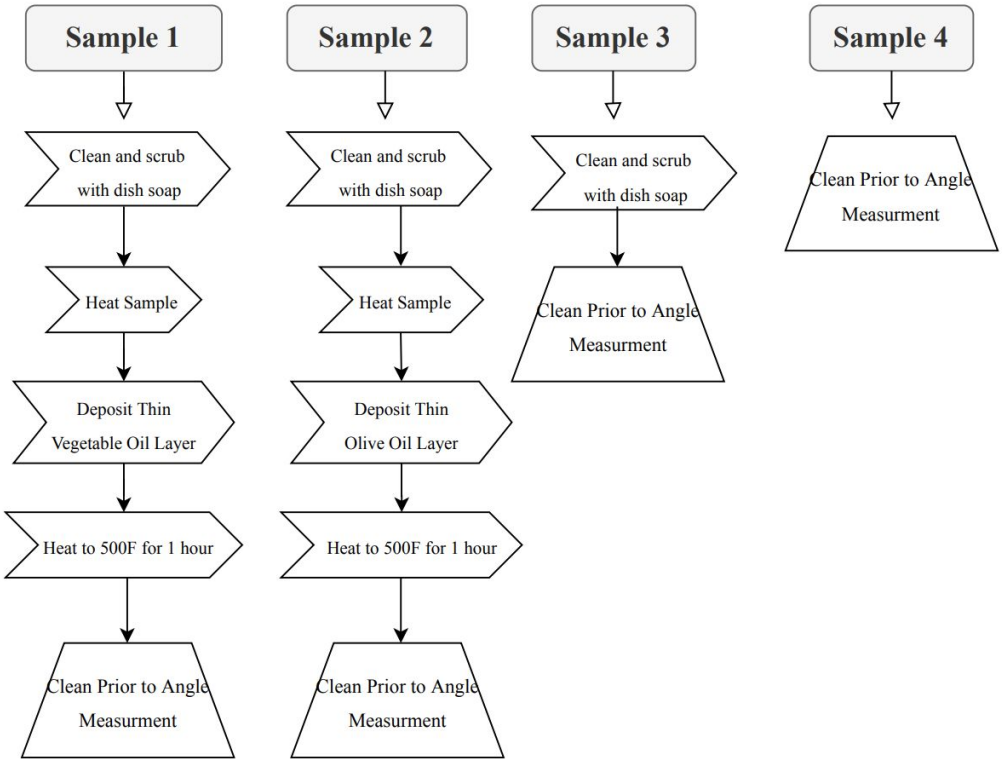

Figure 3. Flowchart of process for each cast iron sample, samples consisting of bare cast iron with vegetable oil, bare cast iron with olive oil, bare cast iron, and cast iron with organic layer intact.

An experiment was conducted testing four different cast iron samples. Some of the samples were exposed to the seasoning treatment and others were left to examine their properties on their own as well as with the organic layer on them already. We also examined the difference between cleaning them prior to measuring the contact angles and not cleaning them. Figure 3

shows the general procedure for all four samples that were tested. Sample 1 and 2 were also subjected to polymerization following the oil layer deposition.

(a)

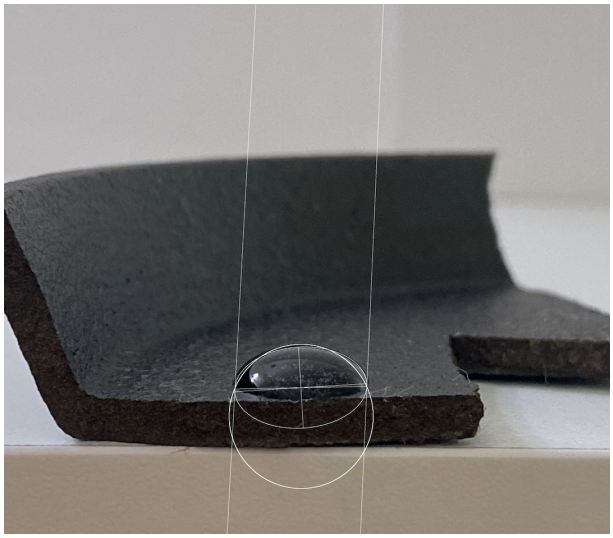

(b)

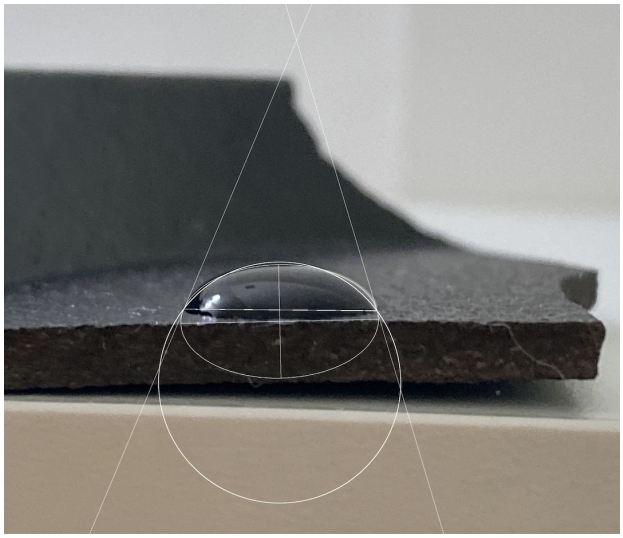

(c)

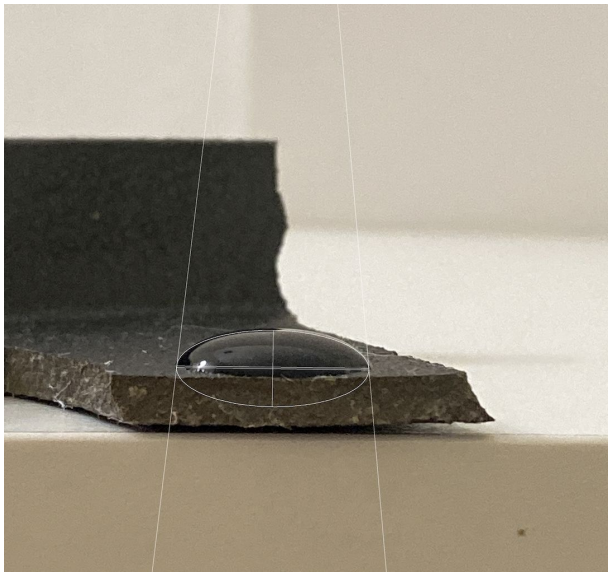

(d)

Figure 4. (a) Contact angle measurement of bare cast iron with vegetable oil treatment. (b) Contact angle measurement of bare cast iron with olive oil treatment. (c) Contact angle measurement of bare cast iron. (d) Contact angle measurement of cast iron with the organic layer.

Figure 4 shows the contact angle measurements of the different cast iron samples that were tested. The measurements were taken with an iPhone 11 as the optical goniometer and with an iPhone 11 as the light source for illumination of the water droplet. The images were then analyzed using ImageJ software and the contact angle plugin. The analysis involves creating ellipses and circles of best fit for each droplet. The tangent lines were also drawn to identify the triple point between the droplet and the surface. The measurements were taken with two base points to identify the contact angle and three points around the droplet to obtain the drop profile. This software allowed us to obtain contact angle measurements, although it did not seem to be the most efficient way. The analysis seemed to give us variable results after several analysis runs, so this led us to believe that it was just an estimation and not an exact measurement.

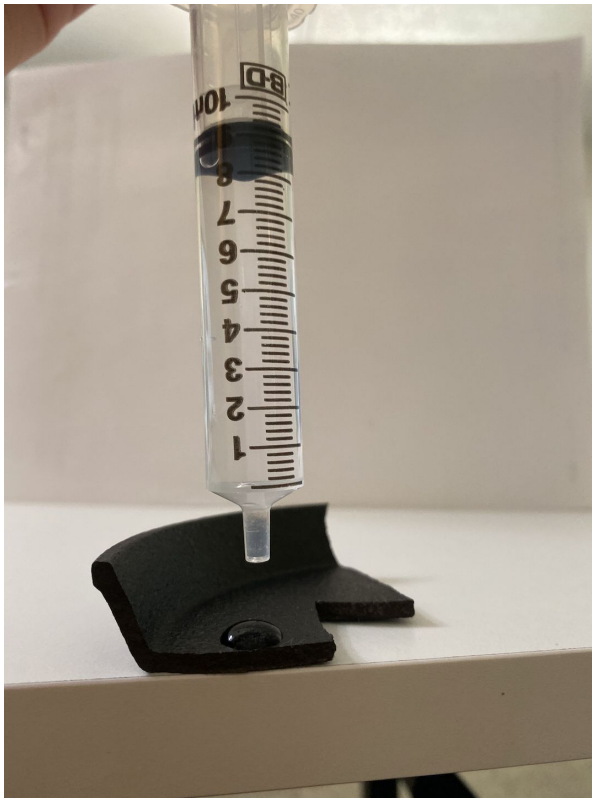

Figure 5. User controlled 10ml syringe to dispense distilled water droplet on cast iron samples.

Figure 5 describes the mechanical process of creating the droplet on the cast iron samples. We used a 10ml syringe to dispense 0.75ml of filtered water. We believed that this method could have been more efficient using a micropipette or a system that dispensed our liquid at a constant pressure and velocity. We found it difficult to exert the same amount of pressure to get the precise volume. Having the volume of the droplet be the same for each sample was critical because this is taken into account via the Young-Laplace equation, which is the partial differential equation that describes the capillary pressure difference across the interface between two static fluids. We also believe our stage setup could have differed as there were some vibrations that could have caused the droplet to move from its original position, as well as the optical system being held manually which resulted in some vibrations from that as well.

Sample	Theta C	Theta Left	Theta Right	Theta E	Radius
Vegetable Oil Cast Iron	113.7	94.2	86.4	86.4	353.95
Olive Oil Cast Iron	127	112.2	106.9	109.6	582.76
Bare Cast Iron	81.3	96.1	95.6	95.8	1623328210
Cast Iron	13.4	102.5	97	99.8	178187624.7

Table 1. Contact angle ellipse and circle measurements via ImageJ contact angle plugin software.

Table 1 demonstrates the calculated angle measurements for each sample. The vegetable oil cast iron and olive oil cast iron samples both indicate that they did have the hydrophobic properties we hypothesized, as their angels were over 90°. The samples that did not undergo the treatment showed less hydrophobic properties, with their angles being less than 90°. Table 1 shows the different angles for each sample, which represent the circle of best fit, ellipse of best fit, left contact angle, right contact angle and the contact angle inside the drop. The contact angle inside the drop would be -180° of each angle found, as this software assumes the drops are

inverted. We believe these measurements show a sufficient correlation but we can also assume that these are estimations and not precise measurements. We can assume this because there were different variables that may have influenced these measurements. When we cleaned the samples prior to measuring the contact angle, we noticed some lint on the samples from the alcohol wipes which could have added to the surface roughness value of each sample. Another reason for the variable data could have been due to uneven coating of the oil when the oil layer was deposited,as the oil was dispensed over the samples and was cleaned as much as possible with a paper towel afterwards. We also believe that the water we used could have had some effect, as it was not DI water as done in previous contact angle experiments (Yuan, 2011).

The cast iron pans, Vegetable Oil Cast Iron and Olive Oil Cast Iron were polymerized at a temperature of 500°F, which was chosen because a temperature around the oil's smoking point would allow for vaporization of the lighter hydrocarbons from the oil layer and leave behind the molecules for polymerization to begin (Canter, 2010). Polymerization is the process of monomers binding with a catalyst, in this case high temperature, to create a polymer. The reaction is an example of chain polymerization, where a chain reaction adds a new monomer unit to the growing polymer molecule one at a time through double or triple bonds in the monomer. The primary steps in chain polymerization is initiation, propagation and termination. In the initiation stage the active free radicals are created and bonds with a double bonded monomer, which also usually requires heat to be present in this reaction. The next step, propagation, is where the consecutive addition of monomers occurs. The final step is termination, where the free radicals react in pairs, which will either occur through combination or disproportionation; this reaction completes the polymer chain.

Procedures:

For our experiment to investigate the contact angle, surface topology, and frictional forces on our surface we must prepare our samples for each instrument. The initial sample preparation that must be done is to obtain our samples and cut them to the proper size for the specific instrument we would be using. We would cut our iron skillet into smaller sections, using a band saw and then sanded down using a 80grit sander. We would then prepare our samples for each specific instrument. We expect the very first sample preparation to be around 10 hours. We would only clean and season the samples that we do not want in order to study the organic layer of it because we need to maintain one of them as our control. For the ones to be stripped of their original organic layer, we would scrub them thoroughly with dish soap and warm water and then dried with a lint free cloth. We would then proceed to take the samples that need to be polymerized and coat them with an oil layer and wipe away any excess oil to ensure we are left with a thin film to be polymerized. We would then proceed to cure the samples in an oven at approximately 500°F for one hour (All about Seasoning). Once the samples have been fully cured and dried, we will prepare them for each instrument. When doing the additional oil layer coatings, we would ensure that each film was evenly layer in order to prevent any additional surface roughness that could alter the measurements. For the oil treatment experiment we would take our cut samples and clean them with anhydrous ethanol and then let them dry before instrument measurements (Yuan, Z.).

For the contact angle instrument we would use an optical contact angle goniometer with a proper light source, sample stage, and mechanical pipet to control the amount of distilled water we are dropping on our samples. The following step is to ensure that all parameters are under control, such as the ambient humidity levels, as this can alter the data we obtain. The experiment would then be followed with data analysis in the Image J software using the contact angle plugin.

For the AFM we would have to make sure our sample is cut to the right size to ensure it would adhere to the substrate for examination and adhere the cast iron sample using carbon cloth tape, where we would then set it to tapping mode because we do not know much about the surface roughness and we also do not want to damage our sample. We would begin with a larger scanner and progressively move to a smaller scanner in order to narrow in on interesting areas we may find to examine the peaks thoroughly. For the SEM we would have to make a cross sectional sample, which we would then polish and ensure it is mounted properly . We can expect the image to be similar to Figure 6.

(a) (b)

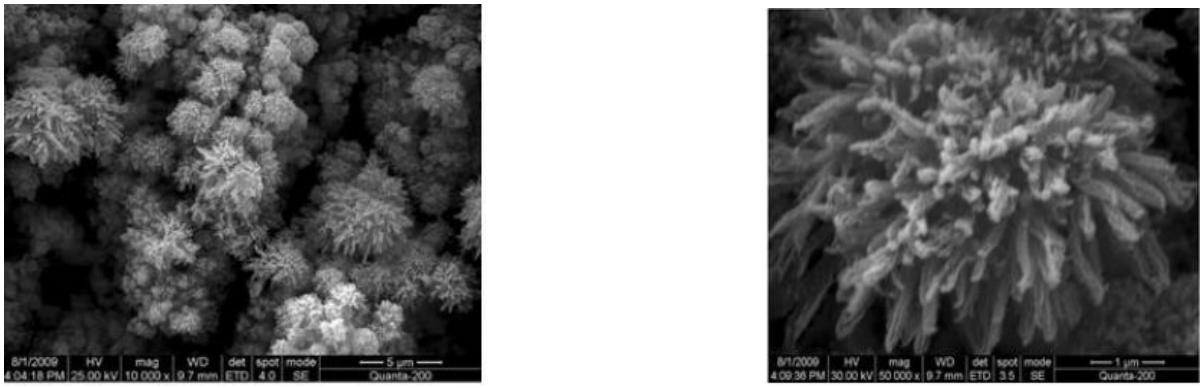

(Yuan, 2011) (Yuan, 2011)

Figure 6. Images of different cast irons treated with different coatings. Figure 6(a) is an untreated common cast iron substrate. Figure 6(b) is a treated cast iron substrate.

The images are examples of imaging that are obtained through SEM. The different seasoned cast irons will each have different images that will be able to give us information on the samples' topography. Changing or modifying the samples changes the microstructure, which we observe in the images above. Using SEM, we also analyze and gain information in the microstructures

and in the process examine contamination or the effect of the oil on the cast iron. Since SEM is such an essential research tool for engineering, by utilizing its ability to detect and analyze surface features of samples, we will be able to gather enough information on our sample.

We will spend time obtaining an efficient cut of our sample to ensure that we are getting an area that accurately represents the entire sample profile. Prior to analyzing, we will also scribe the samples to see how our sample changes when damaged and how the oil layer is responding to that scratch. The scratch will enable us to have good data to analyze when we start looking at our sample on the computer screen. We will be selecting the Through the Lens detector for the SEM to ensure we collect secondary electrons to obtain detailed surface information. For the SEM images, we will be collecting images of the samples before they undergo any polymerization and after to observe any deformation. We will also be taking images at various magnifications to ensure we have a complete image of our sample and see any deformations that would not be seen at a lower magnitude.

Conclusions:

Our research aims to investigate the hydrophobic properties of biopolymer films on cast iron substrates. We intend to analyze how oil treatments on the cast iron substrates change its hydrophobicity properties due to its surface chemistry properties. This research is important as it allows others to have a more concrete idea of what occurs at the molecular level when they decide to season their cookware or add lubricants to the car parts. It is important to understand if there is in fact a difference in adding a polymer film on cast iron substrates for the various applications. Through research conducted by others we have seen how oil treatments have

affected cast iron engine parts and looked at the friction and wear of the cast iron, which will be a component in our investigation. We believe we can begin to answer these hypotheses by obtaining the contact angles before and after oil treatments are applied as well as comparing standardized reference contact angles for cast iron. Using SEM and AFM instruments we will also be able to observe the topography and visibly note any deformations or changes to the cast iron. Some of the sample preparation requirements require us to cut down the cast iron skillet into smaller sections. There would be four pieces of cast iron that will be analyzed, but just two will be seasoned in order to maintain a reference group. One of the cast iron samples will be seasoned with vegetable oil and the other with olive oil. After performing the experiment we will appropriately prepare each sample for imaging according to the guidelines for each instrument. Some of the limitations we expect in our experiment is not having all of the proper equipment and also not having control over each parameter such as the amount of oil deposited or the humidity in the air that could interfere with our measurements. We would also need to have the room free of any vibrations that could interfere with imaging.

The approximate budget for this project is as follows:

a. Sample Preparation: 10 hours (band saw, grinding, polishing, and cleaning)

b. Seasoning Cast Iron: 6 hours (coating, and baking)

c. SEM: 10 hours

d. AFM: 10 hours

e. Contact angle measurements: 5 hours

f. Data analysis: 15 hours

g. Report Preparation: 20 hours

References:

Adli. (2017, October 1). Investigation into Tribological Performance of Vegetable Oils as Biolubricants at Severe Contact Conditions. Retrieved from http://etheses.whiterose.ac.uk/19524/

All About Seasoning. (n.d.). Retrieved from https://www.lodgemfg.com/discover/cleaning-and-care/cast-iron/all-about-seasoning

Canter, S., Newsome, S., Mitch, Kevin, Michael, Elaine, … Tmk. (2010, January 28). Sheryl's Blog. Retrieved from http://sherylcanter.com/wordpress/2010/01/a-science-based-technique-for-seasoning-cast-iron/

Logan, R., Mulheron, M., Jesson, D., & Whiter, J. (2018, August 01). Figure 3: SEM image of cast iron cross section. . Retrieved from https://www.researchgate.net/figure/SEM-image-of-cast-iron-cross-section_fig2_269031105

Pan, S., Zeng, F., Su, N., & Xian, Z. (2019, December 16). The effect of niobium addition on the microstructure and properties of cast iron used in cylinder head. Retrieved April 16, 2020, from http://www.sciencedirect.com/science/article/pii/S2238785419314243)

Petrenec, M., Beran, P., Roupcova, P., & Tesařová, H. (2010, April). Omparison of low cycle fatigue of ductile cast irons with different matrix alloyed with nickel. Retrieved April 24, 2020, from

https://www.researchgate.net/publication/245481547_Comparison_of_low_cycle_fatigue_of_ductile_cast_irons_with_different_matrix_alloyed_with_nickel

Ramachandran, R., & Nosonovsky, M. (2015, August 28). Coupling of surface energy with electric potential makes superhydrophobic surfaces corrosion-resistant. Retrieved from https://pubs.rsc.org/en/content/articlelanding/2015/CP/C5CP04462F#!divAbstract

Razaq, A., Yin, Y., Zhou, J., Shen, X., Ji, X., & Ullah, I. (2019, December 16). *Influence of Alloying Elements Sn and Ti on the Microstructure and Mechanical Properties of Gray Cast Iron*. Retrieved April 15, 2020, from http://www.sciencedirect.com/science/article/pii/S235197891931265X)

Riahi, S., Niroumand, B., Moghadam, A. D., & Rohatgi, P. K. (2018, January 10). Effect of microstructure and surface features on wetting angle of a Fe-3.2 wt%C.E. cast iron with water. Retrieved from https://www.sciencedirect.com/science/article/pii/S0169433217338011

Ruiz-Cabello, J. M., Criado, J. R., Cabrerizo-Vilchez, M., Valverde, M. R., & Vacas, G. (2017, August). *Towards super-nonstick aluminized steel surfaces*. Retrieved April 30, 2020, from http://www.sciencedirect.com/science/article/pii/S0300944016309961

Yoshimoto, T., Matsuo, T., & Ikeda, T. (2019). *The effect of graphite size on hydrogen absorption and tensile properties of ferritic ductile cast iron*. Retrieved April 15, 2020, from http://www.sciencedirect.com/science/article/pii/S2452321619300046)

Yuan, Z., Xiao, J., Wang, C., Zeng, J., Xing, S., & Liu, J. (2011). Preparation of a superamphiphobic surface on a common cast iron substrate. Journal of Coatings Technology and Research, 8(6), 773–777. doi: 10.1007/s11998-011-9365-7

https://link.springer.com/article/10.1007/s11998-011-9365-7

Appendix:

Figure 1. Venn diagram comparing the different techniques that produce different data.

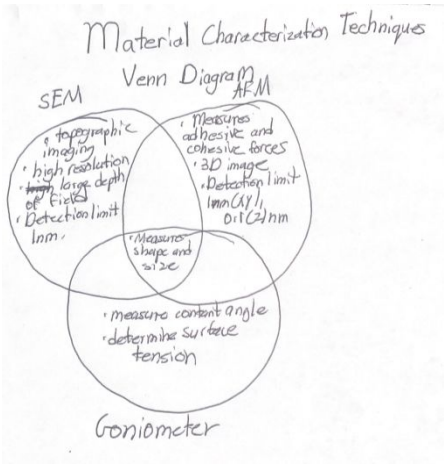

Figure 2. (a) Bare Grey Cast Iron microstructure schematic. (b) Bare Grey Cast Iron after Oil Layer deposition microstructure schematic. (c) Uncleaned Grey Cast Iron with organic layer intact microstructure schematic.

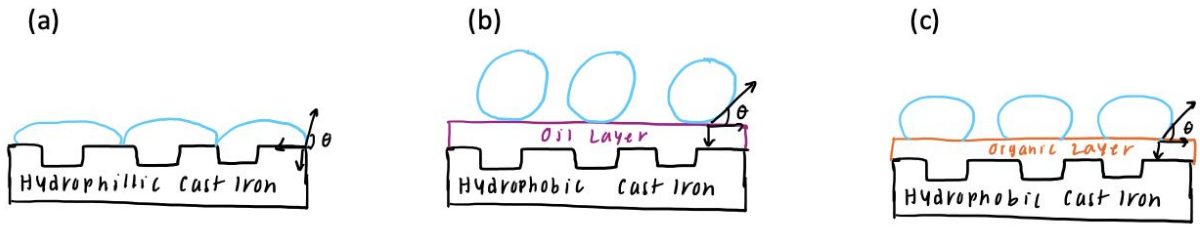

Figure 3. Flowchart of process for each cast iron sample, samples consisting of bare cast iron with vegetable oil, bare cast iron with olive oil, bare cast iron, and cast iron with organic layer intact.

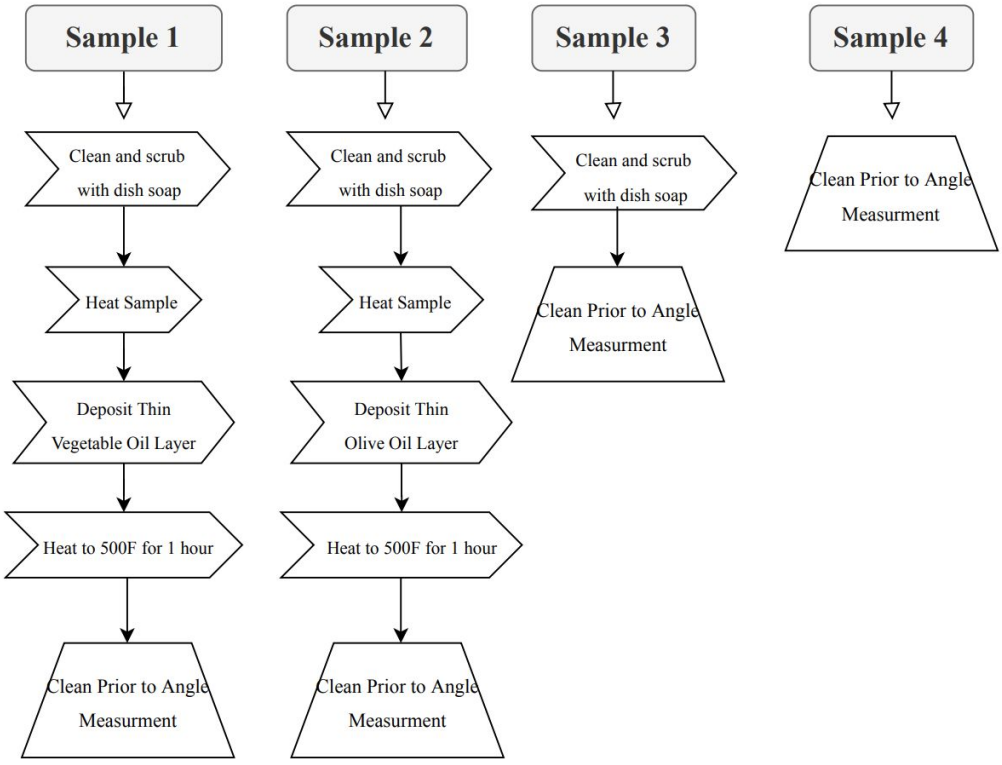

Figure 4. (a) Contact angle measurement of bare cast iron with vegetable oil treatment. (b) Contact angle measurement of bare cast iron with olive oil treatment. (c) Contact angle measurement of bare cast iron. (d) Contact angle measurement of cast iron with the organic layer.

(a) **(b)**

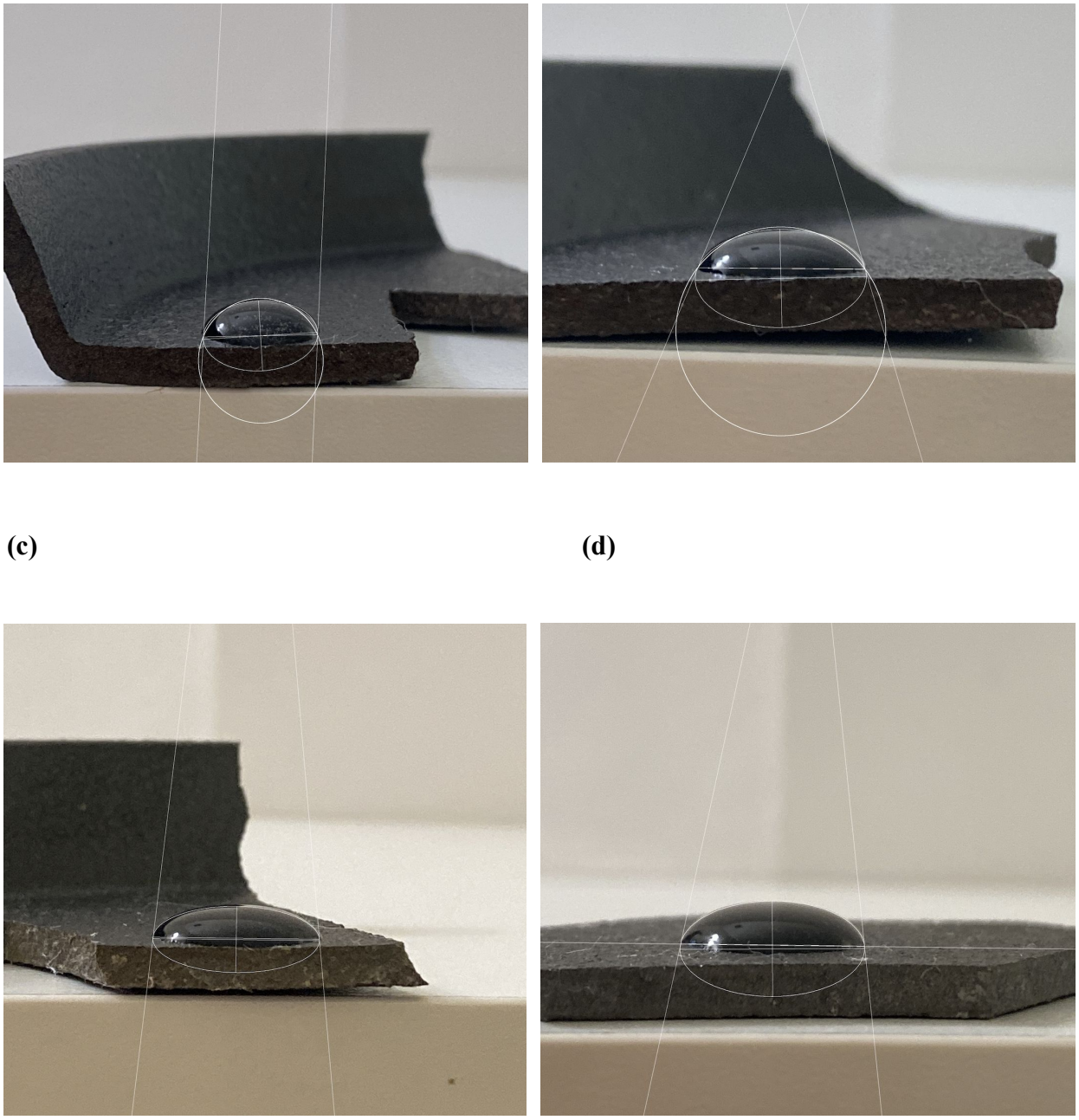

(c) **(d)**

Figure 5. User controlled 10ml syringe to dispense distilled water droplet on cast iron samples.

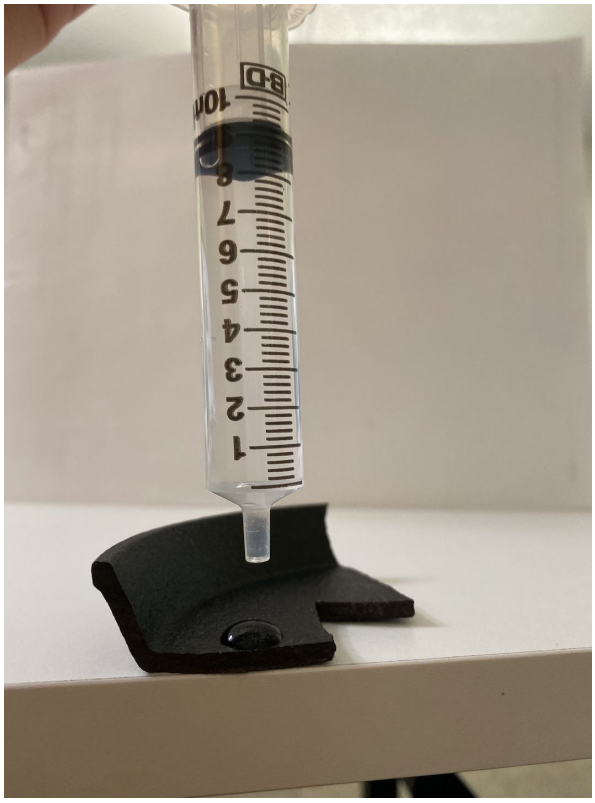

Table 1. Contact angle ellipse and circle measurements via ImageJ contact angle plugin software.

Sample	Theta C	Theta Left	Theta Right	Theta E	Radius
Vegetable Oil Cast Iron	113.7	94.2	86.4	86.4	353.95
Olive Oil Cast Iron	127	112.2	106.9	109.6	582.76
Bare Cast Iron	81.3	96.1	95.6	95.8	1623328210

Cast Iron	13.4	102.5	97	99.8	178187624.7

Figure 6. Images of different cast irons treated with different coatings. Figure 6(a) is an untreated common cast iron substrate. Figure 6(b) is a treated cast iron substrate.

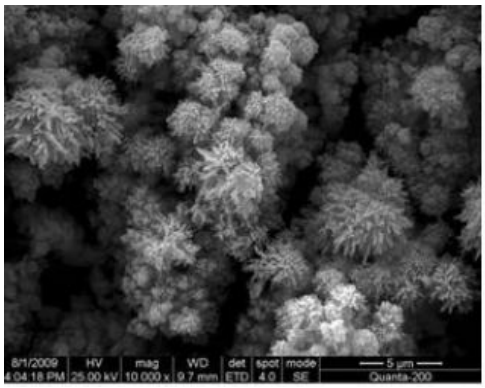

(Yuan, 2011)

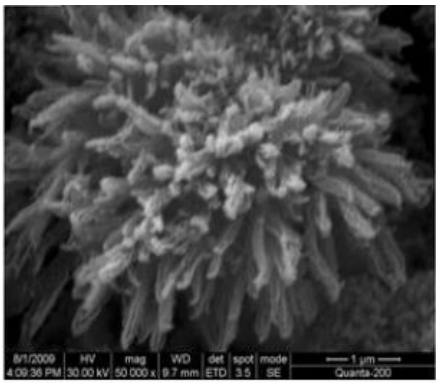

(Yuan, 2011)